



Cite this: *Chem. Sci.*, 2026, **17**, 2148

All publication charges for this article have been paid for by the Royal Society of Chemistry

## Addressing first cycle irreversible capacity in lithium-rich layered oxides by blending with delithiated active materials

Dimitrios Chatzogiannakis,<sup>abc</sup> Violetta Arszelewska,<sup>d</sup> Pierre-Etienne Cabelguen,<sup>d</sup> M. Rosa Palacin  <sup>\*a</sup> and Montse Casas-Cabanas  <sup>\*b,e</sup>

Lithium-rich oxides (LRO), derived from NMC-type materials, are among the most promising next-generation positive electrode candidates for lithium-ion batteries. Despite their potential, their practical application is hindered by inherently low first-cycle coulombic efficiency, caused by the irreversible loss of lithium. In this work, we address this drawback by chemically delithiating secondary active materials –  $\text{LiMn}_2\text{O}_4$  (LMO) or  $\text{LiFePO}_4$  and subsequently blending them with the cobalt-free lithium rich oxide  $\text{Li}_{1.15}\text{Ni}_{0.3}\text{Mn}_{0.55}\text{O}_2$ . The incorporation of these delithiated components improves not only first-cycle efficiency but also capacity retention, with the degree of enhancement proportional to the fraction of added material. Differential scanning calorimetry (DSC) further reveals improved thermal stability for LRO:FePO<sub>4</sub> blends evidenced by a higher decomposition temperature and lower overall heat released. In contrast, blending LRO with  $\lambda\text{-MnO}_2$  blends results in a detrimental effect related to increased moisture sensitivity. *Operando* synchrotron X-ray diffraction on blended electrodes confirms that the secondary active material actively participates in the electrochemical processes. Our findings demonstrate a simple and industry-compatible strategy to mitigate one of the major drawbacks of LROs, paving the way for more sustainable and high performance lithium-ion batteries.

Received 29th August 2025  
Accepted 10th November 2025

DOI: 10.1039/d5sc06660c  
[rsc.li/chemical-science](http://rsc.li/chemical-science)

## Introduction

As efforts towards sustainable transportation intensify, Electric Vehicles (EVs) are becoming increasingly popular. The batteries powering them (predominantly Li-ion) may still benefit from improvement, as this technology was originally developed for portable electronics, which have different performance requirements. Key challenges to meet the requisites of EVs include enhanced safety and improved longevity under sustained high-performance use.

One of the critical components of a Li-ion battery is the positive electrode, often containing layered oxides as active materials. These have a general formula  $\text{LiMO}_2$  where M = Co, Mn, Ni, Al or their combinations. The most representative families are  $\text{LiNi}_x\text{Mn}_y\text{Co}_z\text{O}_2$  where  $x + y + z = 1$ , commonly referred to as NMCs, and  $\text{LiNi}_x\text{Co}_y\text{Al}_z\text{O}_2$  where  $x + y + z = 1$ ,

known as NCAs. Other positive active materials commonly present in commercial batteries are  $\text{LiFePO}_4$  (LFP), with olivine structure, and the spinel  $\text{LiMn}_2\text{O}_4$  (LMO). Each of them offers distinct advantages and drawbacks. In general, layered oxides provide the highest reversible capacities, LFP is recognized for its longest cycle life, safety and cost-effectiveness, and LMO features very fast lithium kinetics while exhibiting low cost, though it generally suffers from lower capacity and shorter cycle life compared to other options.<sup>1,2</sup> To tailor electrode performance to the application needs, blended electrodes combining multiple active materials are often utilized in EV batteries. Yet, its composition is usually decided based on empirical criteria, with few studies attempting to rationalize the interactions between their components.<sup>3–5</sup>

The most commonly used blends contain layered oxides. For instance, when LMO is mixed with NMC it has been observed that, even though the total specific capacity of the electrode decreases, the overall lithium exchange kinetics of the electrode improve. Moreover, such blended electrodes can exhibit additional performance gains due to the synergistic interaction between components, including higher energy density than predicted from the rule of mixture, especially at high rates, and also lower capacity fading, the latter being attributed to suppressed manganese dissolution.<sup>6,7</sup> During cycling, the effective rate experienced by a material within a blend can differ significantly from the nominal cell rate and blend components can

<sup>a</sup>Institut de Ciència de Materials de Barcelona, ICMAB-CSIC, Campus UAB, 08193 Bellaterra, Catalonia, Spain. E-mail: rosa.palacin@icmab.es

<sup>b</sup>Centro de Investigación Cooperativa de Energías Alternativas (CIC energiGUNE), Basque Research and Technology Alliance (BRTA), 01510 Vitoria-Gasteiz, Spain. E-mail: mcasas@cicenergigune.com

<sup>c</sup>ALISTORE-ERI, CNRS FR, 3104, France

<sup>d</sup>UMICORE, 31 rue du Marais, 1000, Brussels, Belgium

<sup>e</sup>Ikerbasque - Basque Foundation for Science, Maria Diaz de Haro 3, 48013 Bilbao, Spain



bear more or less current depending on the state of charge of the cell and the intrinsic reaction kinetics of the active materials.<sup>8</sup>

On the other hand, safety concerns related to EVs mainly revolve around battery related hazards. Malfunction, operation out of specifications and physical abuse of the battery can result in the increase of its temperature, either by heat released from the cell itself or an external heat source (e.g. malfunctioning nearby battery cell). Catastrophic failure typically occurs when the battery exceeds a critical temperature threshold,<sup>9,10</sup> causing a phenomenon known as thermal runaway. During such an event, large amounts of heat are released, triggering a series of exothermic processes that can result in fire, or explosion. The positive electrode plays a crucial role in this phenomenon as its thermal stability and interaction with other components can significantly influence the risk of thermal runaway.<sup>11,12</sup> Additionally, many of the active materials release oxygen when heated, which can fuel combustion in the presence of the flammable organic compounds used as electrolyte solvents in Li-ion batteries.<sup>13</sup> Studies on active materials have been carried out to increase this critical runaway temperature and/or reduce the heat released during the event through chemical substitutions, coatings or electrolyte modification.<sup>14,15</sup> Blending different active materials has also been explored to improve safety in Li-ion batteries.<sup>16</sup>

A very promising family of next-generation positive active materials meant for EVs is the so called lithium-rich layered oxides (LROs).<sup>13,17</sup> Their chemical formula and crystal structure derive from that of layered oxides, yet have a Li/M ratio higher than 1 and can therefore be described as  $\text{Li}_{1+x}\text{M}_{1-x}\text{O}_2$  where typically  $0 < x \leq 0.33$ .<sup>18</sup> These materials offer very large reversible specific capacities able to exceed  $250 \text{ mAh g}^{-1}$ , due to the participation of lattice oxygen in the redox reaction during cycling.<sup>19–21</sup> However, structural changes often involving oxygen release result in significant first-cycle irreversibility, manifesting as low initial coulombic efficiencies (typically around 80%) and poor capacity retention over time. This irreversibility is closely linked to a voltage plateau above 4.5 V during the first battery charge, commonly referred to as “activation”, during which a large amount of lithium is extracted that cannot be completely reaccommodated in the crystal structure upon the subsequent discharge. Thus, there is a fraction of lithium that remains inactive at the negative electrode, which has a detrimental effect to the cell energy density.<sup>22</sup> Additionally, thermal stability is also a major concern, as oxygen loss and structural instability, among other factors, also contribute to a lower onset temperature for thermal decomposition.<sup>23,24</sup>

A limited number of studies have suggested mitigating this loss by incorporating lithium-accepting compounds into positive electrode that can reversibly host lithium ions during cycling. This can be done either by physical blending or as a surface coating. In the seminal work by Gao and Manthiram<sup>25,26</sup> LRO  $\text{Li}[\text{Li}_{0.2}\text{Mn}_{0.54}\text{Ni}_{0.13}\text{Co}_{0.13}]\text{O}_2$  was combined with  $\text{V}_2\text{O}_5$ ,  $\text{Li}_4\text{Mn}_5\text{O}_{12}$  or  $\text{LiV}_3\text{O}_8$  which act as lithium acceptors. These additions enabled reinsertion of lithium into the acceptor after the first charge, thereby reducing the amount of lithium retained in the negative electrode, and therefore the

need for excess graphite. Another similar strategy developed later has been the modification of LRO to form surface and bulk domains of  $\lambda\text{-MnO}_2$  (the delithiated form of LMO)<sup>27–29</sup> or coating with amorphous  $\text{FePO}_4$ . Both strategies were shown to improve the first cycle coulombic efficiency.

In the present work, we introduce a simplified approach that involves blending LRO with a chemically delithiated commercial positive electrode material to act as lithium acceptor, in this case  $\text{FePO}_4$  or  $\lambda\text{-Mn}_2\text{O}_4$ . The composition  $\text{Li}_{1.15}\text{Ni}_{0.3}\text{Mn}_{0.55}\text{O}_2$  was selected (formally within the solid solution between  $\text{Li}_2\text{MnO}_3$  and  $\text{LiNi}_{0.5}\text{Mn}_{0.5}\text{O}_2$ ) as it does not contain any cobalt (toxic and expensive) and delivers high energy density.<sup>30,31</sup> The approach presented herein aims to reduce or eliminate the first-cycle irreversible capacity and enhance the thermal stability of the positive electrode, as presented and discussed in the following sections.

## Results and discussion

### Study of LRO and $\text{FePO}_4$ blended electrodes

Blends of LRO and  $\text{FePO}_4$  were prepared in various weight fractions and electrochemically tested. Fig. 1 shows the voltage vs. capacity profile for the first cycle of cells with LRO: $\text{FePO}_4$  blends, together with their corresponding capacity and coulombic efficiency values. For all compositions, the first

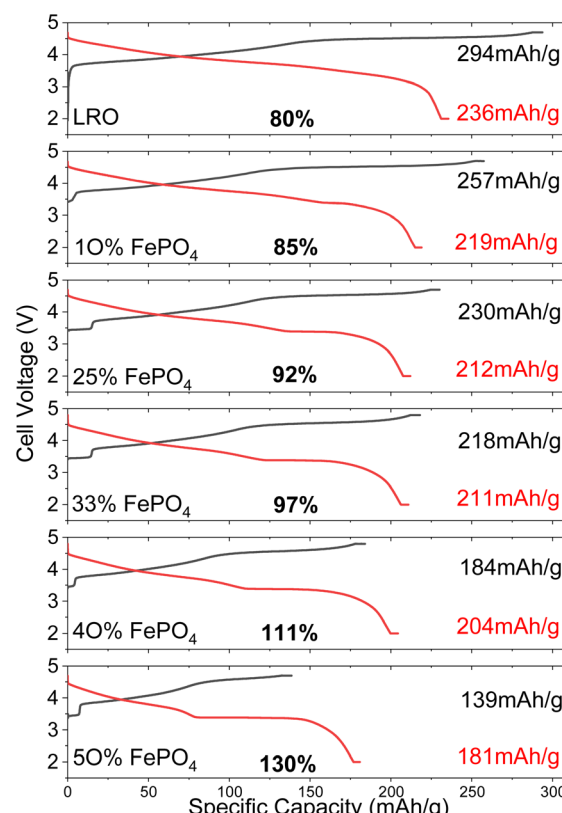


Fig. 1 Voltage vs. capacity curves for the blends of LRO with  $\text{FePO}_4$  with different compositions showing the increase in the first cycle efficiency. First charge (black) and discharge (red) specific capacity values are also included as well as the first cycle coulombic efficiency (bold).



oxidation reveals the high voltage plateau of LRO around 4.6 V with its capacity gradually decreasing as the FePO<sub>4</sub> fraction in the blend increases. Interestingly, blends also showed a small plateau around 3.5 V, which likely indicates the presence of a minor amount of LFP in the electrodes. This feature does not appear to show a trend with fraction blend composition, suggesting possible lithium transfer between materials prior to cycling and/or micro-shorts during assembly. Upon reduction, all cells exhibit a similar voltage *vs.* capacity profile, starting with a sloping region that transitions to a flat plateau around 3.5 V. As the fraction of FePO<sub>4</sub> in the blend increases, the plateau lengthens while the sloping region diminishes.

A similar trend is observed during reduction, where capacity decreases but remains relatively close to the expected values, as shown in Fig. 2. Despite this, the coulombic efficiency improves significantly with blending, with the sample containing 33% FePO<sub>4</sub> achieving an efficiency of almost 100% (Fig. 2). Further increasing FePO<sub>4</sub> content leads to coulombic efficiency values higher than 100%, with a maximum of 130% for 50% weight fraction. It is important to note that in full cells with graphite counter electrodes, the efficiency would not exceed 100%, the higher values achieved in the experiments presented herein are due to the use of lithium metal counter electrodes, which serve as an effectively unlimited lithium source for testing purposes. From the results discussed above it can be inferred that the optimal blend composition for practical applications is 33% FePO<sub>4</sub>, as it balances very high coulombic efficiency with higher capacity than blends with greater FePO<sub>4</sub> content.

The evolution of capacity upon cycling was also studied for cells with 33% FePO<sub>4</sub>, 50% FePO<sub>4</sub> blends and pure LRO as positive electrode active materials. Fig. 3 depicts the evolution of specific capacity for 100 cycles at 1C. The addition of FePO<sub>4</sub>,

results in a significant improvement in capacity retention (after the 100th cycle values were found to be 86% for the pure LRO, 95% for the 33% FePO<sub>4</sub>:LRO blend and 98% for the 50% FePO<sub>4</sub>:LRO).

To evaluate the effect of blending on thermal stability, DSC was performed on oxidized electrodes consisting of pure LRO and a 33% FePO<sub>4</sub>:LRO blend (see Experimental section in the SI). Additionally, two control experiments were conducted: one using a pure FePO<sub>4</sub> electrode, and another consisting only of the inactive components present in the electrode formulation (PVDF and carbon black).

Fig. 4 shows the heat flow as a function of temperature for all electrodes. A sharp exothermic peak is observed for both LRO-containing electrodes, which is tentatively assigned to reactions involving the electrolyte and released O<sub>2</sub> from the electrode.<sup>13,32</sup> The pure LRO sample shows its main process at 224.9 °C with a released heat of 39.2 J g<sup>-1</sup>. On the other hand, the 33% FePO<sub>4</sub> blend shows a peak temperature of 249.7 °C with a significantly reduced released heat (12.5 J g<sup>-1</sup>). These results demonstrate that blending improves thermal stability by raising the decomposition onset temperature by ~25 °C while reducing the released heat by more than two-thirds. In comparison, neither the pure FePO<sub>4</sub> nor the control experiment showed any exothermic processes within the tested range, confirming that the observed reactions originate from the LRO component.

While these DSC results provide valuable insight into the thermal behaviour of the electrodes, it is worth highlighting that, to assertively assess the safety of the electrodes, more rigorous tests are needed using full cells and conditions closer to the ones that more closely replicate commercial batteries. Nonetheless, the observed increase in decomposition temperature and reduction in heat release suggest that blending LRO with FePO<sub>4</sub> may be a promising route toward safer electrode formulations. If these trends are maintained in more application-relevant conditions, blended electrodes could play a significant role in engineering safer batteries.

### Influence of the additive's redox potential

Following the study of LRO blended with FePO<sub>4</sub>, we investigated the effect of an alternative delithiated compound ( $\lambda$ -MnO<sub>2</sub>, the

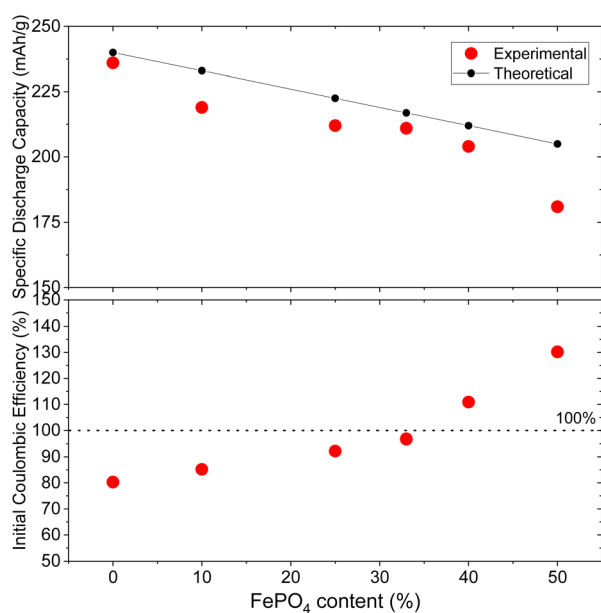


Fig. 2 Experimentally measured and theoretical specific capacities (top), and 1st cycle coulombic efficiencies (bottom) for the studied electrodes. The black points and line show the theoretical capacity of the blends.

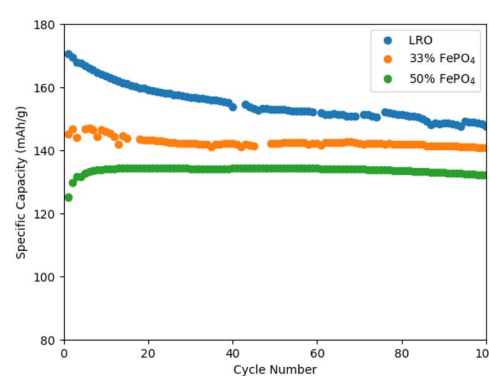


Fig. 3 Evolution of specific capacity during 100 cycles at 1C rate between 2.0 and 4.6 V, for pure LRO (blue), 33% FePO<sub>4</sub>:LRO (orange) and 50% FePO<sub>4</sub>:LRO (green).



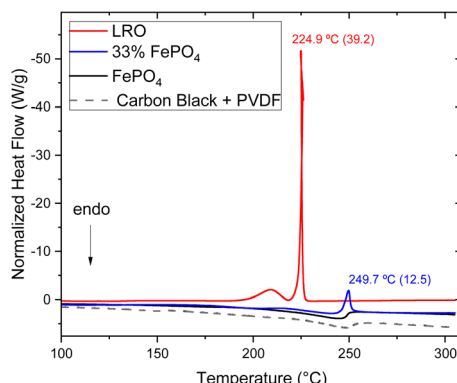


Fig. 4 DSC curves of pure LRO (red line), pure  $\text{FePO}_4$  (black line) and a LRO: $\text{FePO}_4$  blend containing 33%  $\text{FePO}_4$  (blue line). A control experiment is also included (dashed black line) with electrodes containing no active material and only the PVDF binder and carbon black. Heating rate was  $10\text{ }^\circ\text{C min}^{-1}$ .

delithiated form of LMO ( $\text{LiMn}_2\text{O}_4$ ) [30] with a significantly higher operation potential. Indeed, since  $\text{FePO}_4$  exhibits a redox potential around 3.5 V vs.  $\text{Li}^+/\text{Li}$  and LRO starts delithiating at *ca.* 3.7 V vs.  $\text{Li}^+/\text{Li}$ , minimal spontaneous lithium exchange between the two components prior to electrochemical cycling of the electrode is to be expected. In contrast,  $\lambda\text{-MnO}_2$  has a operation potential around 4.1 V vs.  $\text{Li}^+/\text{Li}$ . The operation potentials of  $\text{FePO}_4$  and  $\lambda\text{-MnO}_2$  are shown in Fig. 5 superimposed on the oxidation curve of LRO. At 4.1 V vs.  $\text{Li}^+/\text{Li}$ , LRO is expected to be partially oxidized and hence transfer lithium to  $\lambda\text{-MnO}_2$  is to be expected until equilibrium is reached. The amount of transferred lithium will depend on the relative quantities of the two materials and can significantly affect the electrode's sensitivity to humidity.<sup>33</sup>

To test this hypothesis, two LRO: $\lambda\text{-MnO}_2$  blends with the same weight fractions were prepared, one in ambient conditions and one entirely in an argon filled glovebox with sub-ppm humidity. As seen in Fig. 6, the electrode prepared in air exhibited a significantly lower reversible capacity (88 mAh g<sup>-1</sup>)

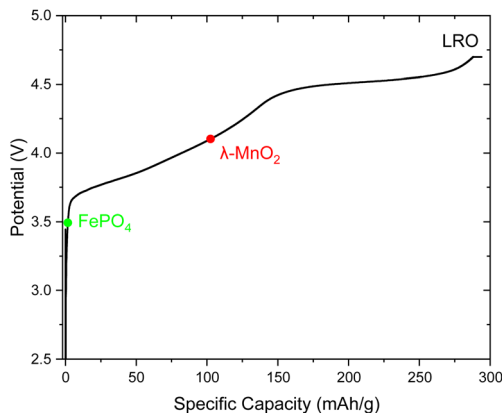


Fig. 5 Potential vs. capacity profile corresponding to the delithiation of LRO, where the relative positions of the operation potentials corresponding to  $\text{FePO}_4$  and  $\lambda\text{-MnO}_2$  are depicted.

while the one prepared in argon delivered 142 mAh g<sup>-1</sup>. The phenomenon is also reflected in the first cycle coulombic efficiency of the electrodes, which were 98% and 79% respectively. Since the increase in the coulombic efficiency is linked to lithium accessible vacancies, failure to increase it could indicate that those sites are already occupied by other species, possibly protons introduced after air exposure. These findings confirm that pre-oxidation of LRO, triggered by the high potential of  $\lambda\text{-MnO}_2$ , can increase its vulnerability to environmental degradation. Preventing moisture exposure is therefore critical if high operation voltage delithiated compounds are to be used.

### Electrode dynamics in LRO: $\text{FePO}_4$ blends

In order to gain further insight into the electrode dynamics in LRO: $\text{FePO}_4$  blends, *operando* synchrotron X-ray diffraction was conducted. Electrodes with three different active material compositions were studied: pure  $\text{FePO}_4$ , and the LRO blends with 33%  $\text{FePO}_4$  and 50%  $\text{FePO}_4$ . Fig. 7a shows the patterns corresponding to their first reduction at C/10 after oxidation to 4.8 V at C/30. At 4.8 V (yellow trace), the characteristic peaks of  $\text{FePO}_4$  are visible with the most intense being the (200) at  $4.8^\circ$ , the (020) at  $8.2^\circ$  and the (121) at  $9.7^\circ$ , which provide a good guide to the eye to follow the reaction. These peaks gradually decrease during reduction, in accordance to the well-known phase transition reaction mechanism  $\text{FePO}_4\text{-LiFePO}_4$ , while new peaks corresponding to  $\text{LiFePO}_4$  gain intensity as lithiation progresses: the (200) peak, around  $4.6^\circ$ , the (020) around  $7.9^\circ$  and the (311) around  $9.4^\circ$ . Peaks corresponding to LRO, exhibit the expected evolution, with the (003) appearing around  $4.9^\circ$  following a non monotonic behaviour, similarly to what is commonly observed in NMC systems. The (101) peak of LRO

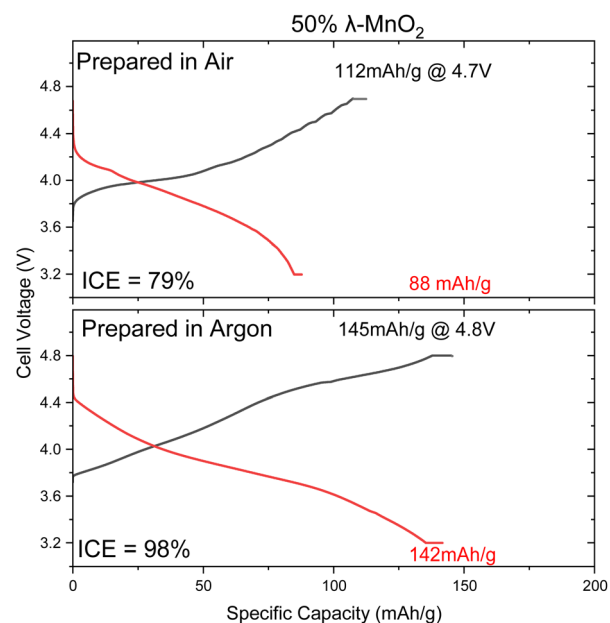


Fig. 6 Voltage vs. capacity profiles of 50% wt. LRO: $\lambda\text{-MnO}_2$  blend prepared either in air (top) or inside an argon filled glovebox. Oxidation curves are depicted in black and reduction curves in red.

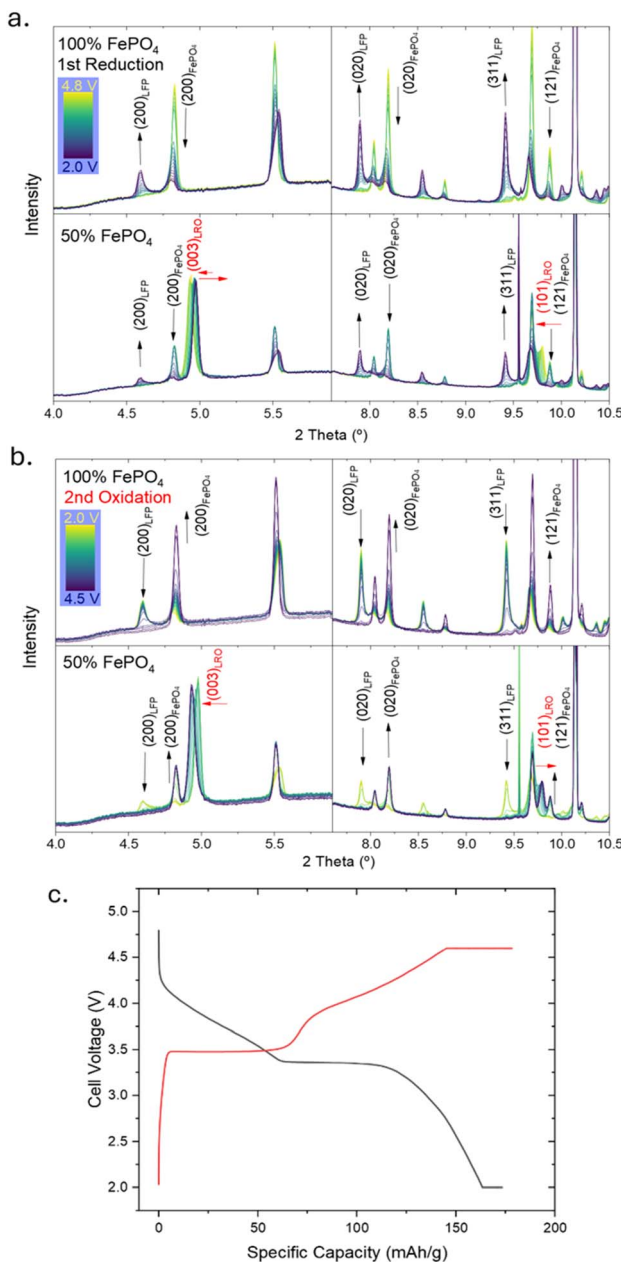


Fig. 7 (a) Evolution of the diffraction patterns for pure FePO<sub>4</sub> and 50% FePO<sub>4</sub>:LRO throughout the first reduction, from yellow line (4.8 V) to blue line (2 V), (b) same plot for the 2nd oxidation from yellow (2 V) to blue line (4.5 V). (c) Specific capacity vs. potential curves of the depicted *operando* experiments.

appears around 9.8° after full oxidation and shifts towards lower angles monotonically during reduction. Fig. 7b shows the patterns of the 2nd oxidation and Fig. 7c the corresponding capacity *vs.* potential curves. The evolution observed is the opposite of that seen during reduction, showing a good structural reversibility of the system. The 33% LRO:FePO<sub>4</sub> blend exhibits a similar behaviour (Fig. S2). The results of these experiments confirm that FePO<sub>4</sub> takes part in the redox activity of the blended electrodes capturing the excess lithium from the LRO.

## Conclusions

A cobalt free, lithium rich layered oxide (LRO) with composition Li<sub>1.15</sub>Ni<sub>0.3</sub>Mn<sub>0.55</sub>O<sub>2</sub> was blended with chemically delithiated active materials, namely FePO<sub>4</sub> and  $\lambda$ -MnO<sub>2</sub> to mitigate first cycle irreversibility and improve thermal stability and capacity retention. Blending with these lithium-acceptor compounds enabled reinsertion of lithium ions during the first charge, thereby reducing the irreversible capacity loss typically associated with the activation process in LRO. For the LRO – FePO<sub>4</sub> system, an optimal blend containing 33% FePO<sub>4</sub> was found to exhibit near zero first cycle irreversible capacity in half cells, better capacity retention, and enhanced thermal stability, with decomposition onset delayed by  $\sim$ 25 °C and a significant reduction in heat release. *Operando* synchrotron X-ray diffraction confirmed the expected activity of FePO<sub>4</sub> validating its redox activity within the electrode and its ability to capture the excess lithium rereleased by the LRO upon the first oxidation. The LRO: $\lambda$ -MnO<sub>2</sub> system appeared to be more complex due to the higher potential of  $\lambda$ -MnO<sub>2</sub>, which induced partial LRO oxidation when mixing. This spontaneous lithium redistribution made the electrode more sensitive to moisture, significantly affecting performance unless handled in a dry atmosphere.

Overall, the results demonstrate that blending LRO with delithiated materials is an effective strategy not only to improve first-cycle efficiency but also to enhance safety and mitigate capacity fading. These findings open a promising path for the rational design of high-energy, safer lithium-ion batteries. Future work should focus on scaling the approach to full-cell configurations and exploring long-term cycling stability under practical operating conditions.

## Author contributions

D. C.: conceptualization, investigation, writing – original draft, writing – review & editing. V. A.: supervision, writing – review & editing. P. E. C.: supervision, writing – review & editing. M. R. P.: conceptualization, supervision, project administration, funding acquisition, writing – original draft, writing – review & editing. M. C. C.: conceptualization, supervision, project administration, funding acquisition, writing – original draft, writing – review & editing.

## Conflicts of interest

There are no conflicts to declare.

## Data availability

Data for this article are available at DIGITAL.CSIC.

Supplementary information is available. See DOI: <https://doi.org/10.1039/d5sc06660c>.

## Acknowledgements

This work has been done in the framework of the doctorate in Materials Science of the Universitat Autònoma de Barcelona and D. C. wants to acknowledge DESTINY MSCA PhD Programme, which has received funding from the European Union's Horizon 2020 research and innovation programme under Grant Agreement No. 945357. ICMAB-CSIC members thank the Spanish Agencia Estatal de Investigación Severo Ochoa Programme for Centres of Excellence in R&D (CEX2023-001263-S) and funding through grant PID2023-146263NB-I00. MCC thanks Grant PID2022-137626OB-C33 funded by MCIN/AEI/10.13039/501100011033 and by "ERDF A way of making Europe" Authors are grateful for access to ALBA synchrotron for beamtime (proposals 2024028311 and 20250330058).

## References

- 1 M. S. Whittingham, Lithium Batteries and Cathode Materials, *Chem. Rev.*, 2004, **104**(10), 4271–4302.
- 2 A. Manthiram, A reflection on lithium-ion battery cathode chemistry, *Nat. Commun.*, 2020, **11**(1), 1550. Available from: <https://www.nature.com/articles/s41467-020-15355-0>.
- 3 M. Casas-Cabanas, A. Ponrouch and M. R. Palacín, Blended Positive Electrodes for Li-Ion Batteries: From Empiricism to Rational Design, *Isr. J. Chem.*, 2021, **61**(1–2), 26–37.
- 4 C. Heubner, T. Liebmann, C. Lämmel, M. Schneider and A. Michaelis, Internal dynamics of blended Li-insertion electrodes, *J. Energy Storage*, 2018, **20**, 101–108.
- 5 D. Chatzogiannakis, O. Arcelus, E. Ayerbe, P. Ghorbanzade, B. Ricci, M. I. De, *et al.*, Key design considerations for blended electrodes in Li-ion batteries, *Solid State Ionics*, 2025, **428**, 116942.
- 6 A. J. Smith, S. R. Smith, T. Byrne, J. C. Burns and J. R. Dahn, Synergies in Blended  $\text{LiMn}_2\text{O}_4$  and  $\text{Li}[\text{Ni}_{1/3}\text{Mn}_{1/3}\text{Co}_{1/3}]_{\text{O}_2}$  Positive Electrodes, *J. Electrochem. Soc.*, 2012, **159**(10), A1696–A1701.
- 7 H. Y. Tran, C. Täubert, M. Fleischhammer, P. Axmann, L. Küppers and M. Wohlfahrt-Mehrens,  $\text{LiMn}_2\text{O}_4$  Spinel/  $\text{LiNi}_{0.8}\text{Co}_{0.15}\text{Al}_{0.05}\text{O}_2$  Blends as Cathode Materials for Lithium-Ion Batteries, *J. Electrochem. Soc.*, 2011, **158**(5), A556.
- 8 D. Chatzogiannakis, M. Fehse, M. A. Cabañero, N. Romano, A. Black, D. Saurel, *et al.*, Towards understanding the functional mechanism and synergistic effects of  $\text{LiMn}_2\text{O}_4$  -  $\text{LiNi}_{0.5}\text{Mn}_{0.3}\text{Co}_{0.2}\text{O}_2$  blended positive electrodes for Lithium-ion batteries, *J. Power Sources*, 2024, **591**, 233804.
- 9 N. E. Galushkin, N. N. Yazvinskaya and D. N. Galushkin, Causes and mechanism of thermal runaway in lithium-ion batteries, contradictions in the generally accepted mechanism, *J. Energy Storage*, 2024, **86**, 111372.
- 10 Y. Dai and A. Panahi, Thermal runaway process in lithium-ion batteries: A review, *Next Energy*, 2025, **6**, 100186.
- 11 D. Doughty and E. P. Roth, A General Discussion of Li Ion Battery Safety, *Electrochem. Soc. Interface*, 2012, **21**, 37–44.
- 12 R. C. Shurtz and J. C. Hewson, Review—Materials Science Predictions of Thermal Runaway in Layered Metal-Oxide Cathodes: A Review of Thermodynamics, *J. Electrochem. Soc.*, 2020, **167**(9), 090543.
- 13 J. Hou, X. Feng, L. Wang, X. Liu, A. Ohma, L. Lu, *et al.*, Unlocking the self-supported thermal runaway of high-energy lithium-ion batteries, *Energy Storage Mater.*, 2021, **39**, 395–402.
- 14 H. Yang, H. Wu, M. Ge, L. Li, Y. Yuan, Q. Yao, *et al.*, Simultaneously Dual Modification of Ni-Rich Layered Oxide Cathode for High-Energy Lithium-Ion Batteries, *Adv. Funct. Mater.*, 2019, **29**(13), 1808825. Available from: <https://onlinelibrary.wiley.com/doi/10.1002/adfm.201808825>.
- 15 R. W. Schmitz, P. Murmann, R. Schmitz, R. Müller, L. Krämer, J. Kasnatscheew, *et al.*, Investigations on novel electrolytes, solvents and SEI additives for use in lithium-ion batteries: Systematic electrochemical characterization and detailed analysis by spectroscopic methods, *Prog. Solid State Chem.*, 2014, **42**(4), 65–84.
- 16 G. Sun, S. Lai, X. Kong, Z. Chen, K. Li, R. Zhou, *et al.*, Synergistic Effect between  $\text{LiNi}_{0.5}\text{Co}_{0.2}\text{Mn}_{0.3}\text{O}_2$  and  $\text{LiFe}_{0.15}\text{Mn}_{0.85}\text{PO}_4/\text{C}$  on Rate and Thermal Performance for Lithium Ion Batteries, *ACS Appl. Mater. Interfaces*, 2018, **10**(19), 16458–16466.
- 17 P. Rozier and J. M. Tarascon, Review—Li-Rich Layered Oxide Cathodes for Next-Generation Li-Ion Batteries: Chances and Challenges, *J. Electrochem. Soc.*, 2015, **162**(14), A2490–A2499.
- 18 W. Zuo, M. Luo, X. Liu, J. Wu, H. Liu, J. Li, *et al.*, Li-rich cathodes for rechargeable Li-based batteries: reaction mechanisms and advanced characterization techniques, *Energy Environ. Sci.*, 2020, **13**(12), 4450–4497.
- 19 G. Assat and J. M. Tarascon, Fundamental understanding and practical challenges of anionic redox activity in Li-ion batteries, *Nat. Energy*, 2018, **3**(5), 373–386.
- 20 H. Y. Jang, D. Eum, J. Cho, J. Lim, Y. Lee, J. H. Song, *et al.*, Structurally robust lithium-rich layered oxides for high-energy and long-lasting cathodes, *Nat. Commun.*, 2024, **15**(1), 1288. Available from: <https://www.nature.com/articles/s41467-024-45490-x>.
- 21 M. Zhang, D. A. Kitchaev, Z. Lebens-Higgins, J. Vinckeviciute, M. Zuba, P. J. Reeves, *et al.*, Pushing the limit of 3d transition metal-based layered oxides that use both cation and anion redox for energy storage, *Nat. Rev. Mater.*, 2022, **7**(7), 522–540.
- 22 T. Lin, T. Seaby, Y. Hu, S. Ding, Y. Liu, B. Luo, *et al.*, Understanding and Control of Activation Process of Lithium-Rich Cathode Materials, *Electrochem. Energy Rev.*, 2022, **5**(S2), 27.
- 23 Z. Deng, Y. Liu, L. Wang, N. Fu, Y. Li, Y. Luo, *et al.*, Challenges of thermal stability of high-energy layered oxide cathode materials for lithium-ion batteries: A review, *Mater. Today*, 2023, **69**, 236–261.
- 24 H. Pan, S. Jiao, Z. Xue, J. Zhang, X. Xu, L. Gan, *et al.*, The Roles of Ni and Mn in the Thermal Stability of Lithium-Rich Manganese-Rich Oxide Cathode, *Adv. Energy Mater.*, 2023, **13**(15), 2203989. Available from: <https://onlinelibrary.wiley.com/doi/10.1002/aenm.202203989>.



25 J. Gao and A. Manthiram, Eliminating the irreversible capacity loss of high capacity layered Li  $[Li0.2Mn0.54Ni0.13Co0.13]O_2$  cathode by blending with other lithium insertion hosts, *J. Power Sources*, 2009, **191**(2), 644–647.

26 J. Gao, J. Kim and A. Manthiram, High capacity Li  $[Li0.2Mn0.54Ni0.13Co0.13]O_2$ –V<sub>2</sub>O<sub>5</sub> composite cathodes with low irreversible capacity loss for lithium ion batteries, *Electrochem. Commun.*, 2009, **11**(1), 84–86.

27 L. Zhou, Z. Yin, Z. Ding, X. Li, Z. Wang and Y. Wang, Bulk and surface reconstructed Li-rich Mn-based cathode material for lithium ion batteries with eliminating irreversible capacity loss, *J. Electroanal. Chem.*, 2018, **829**, 7–15.

28 X. Hu, H. Guo, J. Wang, Z. Wang, X. Li, Q. Hu, *et al.*, Structural and electrochemical characterization of NH<sub>4</sub>F-pretreated lithium-rich layered Li  $[Li0.2Ni0.13Co0.13Mn0.54]O_2$  cathodes for lithium-ion batteries, *Ceram. Int.*, 2018, **44**(12), 14370–14376.

29 J. Zheng, S. Deng, Z. Shi, H. Xu, H. Xu, Y. Deng, *et al.*, The effects of persulfate treatment on the electrochemical properties of Li  $[Li0.2Mn0.54Ni0.13Co0.13]O_2$  cathode material, *J. Power Sources*, 2013, **221**, 108–113.

30 Z. Lu, D. D. MacNeil and J. R. Dahn, Layered Cathode Materials Li  $[NixLi(1/3 - 2x/3)Mn(2/3 - x/3)]O_2$  for Lithium-Ion Batteries, *Electrochem. Solid-State Lett.*, 2001, **4**(11), A191.

31 C. S. Johnson, J. S. Kim, C. Lefief, N. Li, J. T. Vaughney and M. M. Thackeray, The significance of the Li<sub>2</sub>MnO<sub>3</sub> component in ‘composite’  $xLi_2MnO_3 \cdot (1-x) LiMn0.5Ni0.5O_2$  electrodes, *Electrochem. Commun.*, 2004, **6**(10), 1085–1091.

32 Z. Zhang, D. Fouchard and J. R. Rea, Differential scanning calorimetry material studies: implications for the safety of lithium-ion cells, *J. Power Sources*, 1998, **70**(1), 16–20.

33 P. Xu, X. Guo, B. Jiao, J. Chen, M. Zhang, H. Liu, *et al.*, Proton-exchange induced reactivity in layered oxides for lithium-ion batteries, *Nat. Commun.*, 2024, **15**(1), 9842.

